Research Article | Vol. 11, No. 4 / 1 April 2020 / Biomedical Optics Express 2178
Biomedical Optics EXPRESS

Thermographic detection and quantification of THC in oral fluid at unprecedented low concentrations

DAMBER THAPA,[1,2] NAKISA SAMADI,[1,2] NISARG PATEL,[1] AND NIMA TABATABAEI[1,*]

[1]Department of Mechanical Engineering, Lassonde School of Engineering, York University, 4700 Keele St., Toronto, ON, M3J 1P3, Canada
[2]Equal contribution
[*]Nima.Tabatabaei@Lassonde.YorkU.ca

Abstract: With recent changes in the legalization of cannabis around the world, there is an urgent need for rapid, yet sensitive, screening devices for testing drivers and employees under the influence of cannabis at the roadside and at the workplace, respectively. Oral fluid lateral flow immunoassays (LFAs) have recently been explored for such applications. While LFAs offer on-site, low-cost and rapid detection of tetrahydrocannabinol (THC), their nominal detection threshold is about 25 ng/ml, which is well above the 1-5 ng/ml *per se* limits set by regulations. In this paper, we report on the development of a thermo-photonic imaging system that utilizes the commercially available low-cost LFAs but offers detection of THC at unprecedented low concentrations. Our reader technology examines photothermal responses of gold nanoparticles (GNPs) in LFA through lock-in thermography (LIT). Our results (n = 300) suggest that the demodulation of localized surface plasmon resonance responses of GNPs captured by infrared cameras allows for detection of THC concentrations as low as 2 ng/ml with 96% accuracy. Quantification of THC concentration is also achievable with our technology through calibration.

1. Introduction

Cannabis and its byproducts are the most widely used psychoactive substances worldwide [1]. According to the World Health Organization, about 147 million people, 2.5% of the world population, consume cannabis [2], and yet this number is expected to increase in the wake of the recent legalization of Cannabis in Europe and North America [3]. While cannabis affects people differently, most studies suggest that consuming cannabis impairs coordination, memory, associative learning, attention, cognitive flexibility, and, to a certain degree, the reaction time of users [4]. More importantly, cannabis impairment is found to be highly correlated with driving skills; the higher the impairment, the worse the driving-related skills [5]. Accordingly, the risk of fatal accidents is significantly increased while driving under the influence of cannabis [6–7] and since young adults are the most frequent users of cannabis in Europe and North America [8–9], cannabis is believed to be an important contributor to the elevated risk of motor vehicle accidents in younger populations [10–13].

With widespread worldwide trends in the legalization of cannabis, driving a motor vehicle while impaired has become a pressing matter for governments. Many jurisdictions in Europe and North America have recognized the urgent need to regulate the impairment aspects of the legalization of cannabis and formalized that operating a motor vehicle while impaired is prohibited. However, since the determination of impairment is not a straightforward matter, regulating bodies has established *per se* limits for the concentration of Tetrahydrocannabinol (THC; a principal psychoactive element of cannabis) as a key measure in determining impairment. Existing *per se* limits for THC are defined in the whole blood/plasma and vary widely between

#388990 https://doi.org/10.1364/BOE.388990
Journal © 2020 Received 23 Jan 2020; revised 11 Mar 2020; accepted 14 Mar 2020; published 24 Mar 2020

Biomedical Optics EXPRESS

jurisdictions (1 to 5 ng/ml). Nonetheless, accurate measurement of THC in blood has proven to be challenging as withdrawal of blood samples need to take place in medical facilities, causing a significant delay in sampling (usually 1-2 hours) during which THC concentration in the blood dramatically drops [14]. To overcome this systematic source of error in screening, and allow for proper enforcement of regulations, law enforcement in most jurisdictions have advocated and, even regulated, the use of devices that screen and measure THC in accessible bodily fluids such as oral fluid [15]. Screening THC in oral fluid allows for easy collection of samples in public and provides rapid analysis without the need for sophisticated equipment and highly trained/medical personnel. Studies suggest a close correlation between the concentration of THC in blood and oral fluid, especially about half an hour after consumption [16].

Reliable screening and measurement of THC in the workplace is another pressing need in the wake of the legalization of cannabis; especially since cannabis is the most commonly found drug among workers in many countries [17–21]. While the burden of proof for detecting THC in the workplace is, normally, lower than that of roadside, workplace safety is by far a larger need, encompassing the majority of the 3.1 billion USD global market of drug of abuse testing. Workplace safety field studies suggest that acute intoxication from cannabis smoking significantly impair employees' performance, leading to increased risks of work-related accidents [22]. Traditionally, urinalysis testing has been the choice for testing drugs in the workplace. However, studies suggest that urine tests have poor validity and low sensitivity to detect employees who represent a safety risk mostly because (1) THC has a long half-life of elimination in urine and can be detected in urine up to weeks after last use among heavy users, occluding the correlation between urinalysis positive test and impairment at time of sample collection. (2) the privacy considerations in collecting urine samples allow for tampering with sample collection, jeopardizing the validity of urine test results.

Irrespective of market (workplace vs roadside), laboratory-based analytical techniques based on chromatographic separation procedures, such as gas chromatography-mass spectrometry (GC-MS) [23], gas chromatography-tandem mass spectroscopy (GC-MS/MS) [24], liquid chromatography-tandem mass spectrometry (LC-MS/MS) [25], high-performance liquid chromatography (HPLC) [26], are considered as the gold standard for detecting and quantifying THC. While these laboratory-based methods are highly sensitive and specific for cannabinoid detection, they are expensive, complex and laborious because they not only involve lengthy sample preparation and chromatographic separation procedures but also are, normally, carried out by highly trained personnel in a controlled laboratory environment. Long turnaround time is another limitation of laboratory-based analytical methods because in most scenarios impaired person needs to be immediately identified and isolated in order to prevent immediate acute events. To overcome the challenges of THC screening in blood and urine, technologies testing oral fluids using affinity chromatography methods, such as lateral flow immunoassays (LFAs), have recently been explored both at the workplace and roadside [27–28]. Oral fluid LFA technologies offer simple, low-cost, portable, and rapid detection of THC. However, the detection threshold of THC in commercially available LFAs is normally limited to greater than 25 ng/ml, which is insufficient for proper enforcement of workplace and roadside *per se* regulations.

In this manuscript, we demonstrate how thermographic interrogation of commercially-available low-cost oral fluid LFAs with a nominal detection limit of 25ng/ml can offer an order of magnitude improvement in detection limit, enabling reliable detection and quantification of THC at concentrations as low as 2ng/ml. Interpretation of LFAs is, normally, carried out either visually or using a reader based on the intensity of visible-light scattering from immobilized gold nanoparticles (GNPs). Our innovation [29], on the other hand, explores the light absorption thermal signatures of GNPs in response to modulated laser illumination [30] in order to minimize background noise levels and improve detection performance. Our results ($n = 300$) suggest that the demodulation of thermal-wave responses of GNPs through lock-in demodulation of

Biomedical Optics EXPRESS

radiometric signals registered by infrared cameras (aka. Lock-In Thermography; LIT) allows for detection of THC concentrations as low as 2 ng/ml with an accuracy of 96%. Another key differentiator of our technology is its ability to reliably quantify THC concentration using commercially available and low-cost LFAs through calibration. In this manuscript, we also offer and discuss the statistical comparison of the detection performance of developed technology against those of human visual interpretation.

2. Methods

2.1. Lateral flow immunoassay

Lateral flow immunoassays are simple paper-based devices used for point-of-care diagnostics in a broad spectrum of fields, spanning from agriculture to medicine to food and environmental testing. A typical LFA strip consists of four major components; sample pad, conjugate release pad, detection zone, and absorbent pad, all mounted on a plastic backing card as shown schematically in Fig. 1(a).

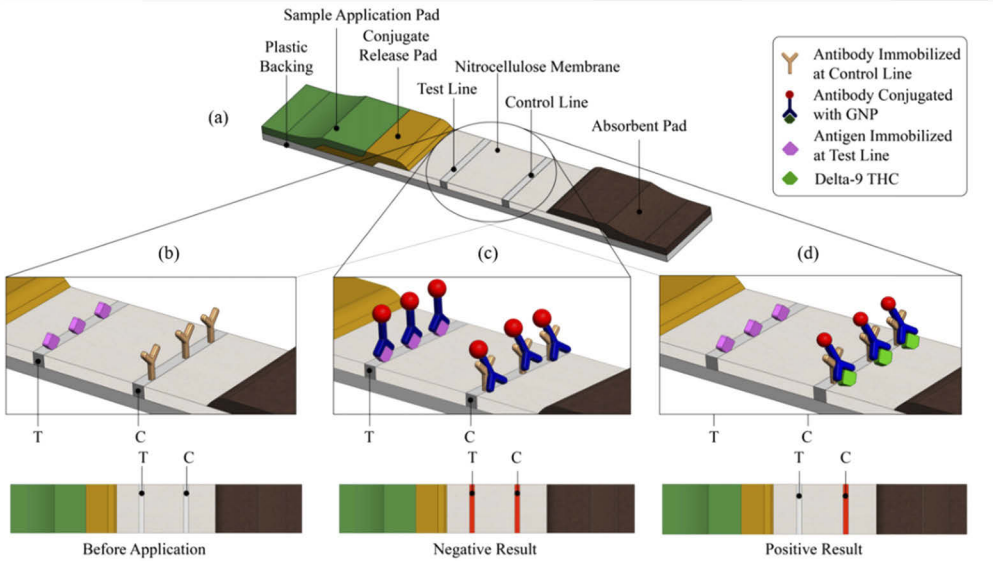

Fig. 1. (a) Schematic diagram of LFA test strip. Schematic illustration of binding mechanisms of competitive LFAs (b) before use, (c) negative test, and (d) positive test with their respective visual appearance.

For detection of small size analytes such as THC, a competitive LFA format, in which an increase in analyte concentration yields reduction of color intensity in test band, is often used. In such design, the sample (e.g., oral fluid) applied at the sample pad migrates into the conjugate release pad that contains the primary antibody conjugated to the colored particles (usually GNPs). An antibody is a special type of protein responsible for binding to specific antigens or other molecules during immunoassay. Based on their binding capability, they are broadly divided into primary and secondary antibodies. Primary antibodies are those antibodies that bind to other antibodies, antigen or any other substance of interest, whereas secondary antibodies are those antibodies that bind to primary antibodies. Antigens are typically proteins peptides, or polysaccharides, responsible for binding to antibodies to form an antigen-antibody complex. Therefore, during the immunoassay, the primary antibody-GNP conjugates attach to analyte in the conjugate release pad and flow along the strip to enter the detection zone. The detection zone consists of antigen immobilized at the test band and secondary antibody immobilized at the

Biomedical Optics EXPRESS

control band. The antigen has the ability to bind with the primary antibody while the secondary antibody has the ability to bind with labeled antibody conjugate. Small analytes, such as THC have a single antigenic determinant and hence cannot bind to two antibodies simultaneously. Therefore, if the analyte is present in the sample it binds with the primary antibody and hence blocks the binding between the antigen and primary antibody, resulting in absence of color in the test band. On the other hand, if the target analyte is absent, the primary antibody binds to the antigen immobilized in the test band and a strong color line is seen in the test band (negative test). The presence of the control line ensures that the test is performed correctly. Figures 1(b) and 1(c) and 1(d), schematically, show binding mechanism and visual presentation of LFA for blank, negative and positive tests in competitive LFA design. The absorbent pad absorbs the excess sample and prevents the backflow of the liquid [31]. In this study, commercially available oral fluid LFA strips for detection of THC (NarcoCheck saliva test strips, Kappa city Biotech SAS, Montluçon, France) with a nominal detection limit of 25ng/ml were used.

2.2. Preparation of oral fluid-THC solutions and LFA test strips

To examine the response of our technology to different concentrations of THC in oral fluid, the standardized recipe of the Canadian Society of Forensic Science Drugs and Driving Committee was followed [32]. That is, a known volume of Delta-9 THC stock solution (MilliporeSigma; Oakville, Canada) was mixed with non-stabilized artificial saliva (Pickering Laboratories, Inc, Mountain View, California, USA) to attain the desired THC concentrations of 25, 10, 7.5, 5, 2 and 0 ng/ml. To study the reproducibility, ten (10) LFAs were spiked with 150µl of solution at each THC concentration. The LFA strips were then interpreted by visual and LIT methods.

2.3. Lock-in thermography interpretation of LFAs

A schematic of the custom-made lock-in thermography system used in this study is depicted in Fig. 2(a). While detailed information about the system can be found elsewhere [33–36], in short, an intensity-modulated near-infrared light (808nm Multimode Pumping Fiber Coupled Laser Diode, Hangzhou Brandnew Technology Co., Ltd, Hangzhou, China) was collimated (F220SMA-780 collimator, Thorlabs Inc, Newton, USA), homogenized (ED1-C20-MD diffuser, Thorlabs Inc, Newton, USA), and impinged onto the sample (Fig. 2(a)). A multifunctional data acquisition unit (National Instruments, Austin, Texas, NI USB-6001) was used to modulate the laser intensity at the desired modulation frequency. Here, we used 1Hz laser modulation frequency to illuminate the sample. The average optical intensity on the sample surface was 2.7 W/cm^2. Radiometric detection was synchronously carried out via a long-wave infrared camera (Xenics Gobi 640, Belgium, spectral range 8-14µm) at 100 frames per second through a frame grabber (Euresys, Angleur, Belgium, Grablink Full) and via Cameralink interface. A 24 mm focal-length objective lens was used to focus the camera on the surface of the LFAs. Lock-in demodulation of acquired thermal camera signals was performed in the LabVIEW environment to obtain the amplitude of ensuing thermal waves at each pixel [33–36].

MATLAB software (MathWorks, Version R2017a) was used for analyzing the amplitude images. A representative amplitude image is shown in Fig. 2(b). The analysis software calculates the average intensity of pixels over all the columns in a strip, as shown in Fig. 2(c). To minimize the systematic errors induced by day-to-day variations in laser illumination system and manufacturing of LFAs, the contrast of LFA test strips in amplitude image were normalized by scaling the image contrast between those of the surrounding white nitrocellulose paper (red rectangle in Fig. 2(b)) and control line. After normalization, the average intensity of pixels over all the columns in a strip was calculated, which generated two bell-shaped curves at the control and test bands, as shown in Fig. 2(c). For quantitative analysis, a metric was defined as the average of the amplitude values within the full width at half maximum (FWHM) of the test line curve (between points A and B

Biomedical Optics EXPRESS

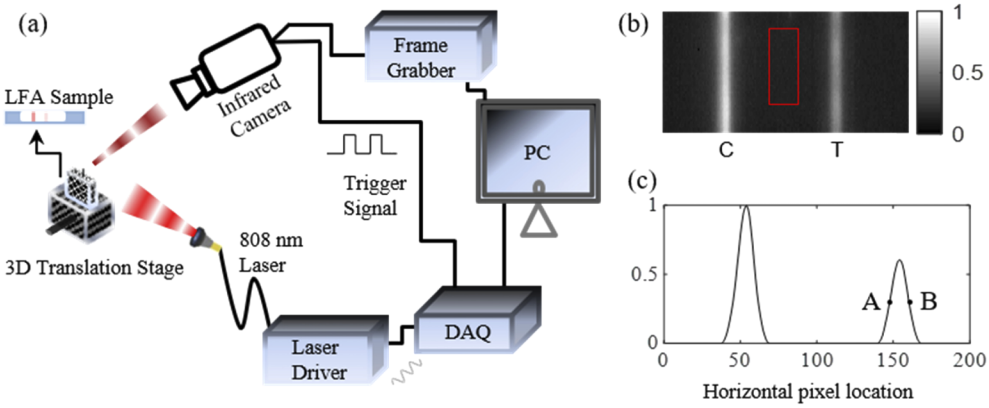

Fig. 2. (a) A schematic diagram of the LIT imaging system used for the interpretation of LFA test strips. (b) Amplitude image after LIT measurement. (c) Average intensity of pixels over all the columns in a strip.

in Fig. 2(c)). Throughout this manuscript, we will adopt this metric as a normalized amplitude value and use it for calibration and quantitative comparison of LFAs at different concentrations.

2.4. Visual interpretation of LFAs

Thirty-two students at York University, 20–35 years old, were recruited for visual interpretation of LFA strips spiked at various THC concentrations (0-25 ng/ml). Since LFA strips consisted of colored test and control lines, the Ishihara color vision test was administered to each participant to screen for color vision deficiencies. Subjects were excluded if they did not pass the Ishihara color vision test and/or had any history of ocular disease/surgery. Two participants out of 32 could not pass the Ishihara color vision test, so they were excluded from the study. All participants had a normal or corrected-to-normal vision and reported no visual disorders or impairments. All studies were conducted in a room with normal lighting condition and participants were asked to perform two tasks. In the first task, participants were asked to interpret the test results, such as positive, negative and invalid in accordance with the LFA manufacturer instruction. The second task was focused on screening the ability of participants to sort LFAs based on the concentration of THC. To do so, 2 LFAs from each concentration of THC were randomly selected as reference visual guide for participants. These reference LFAs were represented to participants as bins. Only investigators were aware of the concentration of THC at each bin. In the following text, we will identify the bins as bins 1-6 corresponding to THC concentrations of 0, 2, 5, 7.5, 10 and 25 ng/ml, respectively. After the preparation of bins, visual assessments of participants were tested using the remaining 8 LFAs at each concentration. That is, the remaining 48 test LFAs (6 concentrations $\times$ 8 LFAs at each concentration) were shuffled and placed in a container. Then, participants were asked to pick up test LFAs one-by-one, compare the test LFA against all reference bins, then place the test LFA in the bin that they think best matches the test LFA. To minimize the subjective bias (memorization), the positions of the reference LFAs and corresponding bins were randomized 3 times (every 1/3 of the total LFAs) during each study. The test was repeated for all the spiked LFA test strips with all the 30 participants, resulting in 1,440 (48×30) data points. This study was approved by the office of the research ethics committee at York University (certificate #: e2019-006) and was conducted according to the Declaration of Helsinki.

Biomedical Optics EXPRESS

2.5. Data analysis

The one-way analysis of variance (ANOVA) was used to determine whether there were any statistically significant differences in mean normalized amplitude values between different concentration groups. If the ANOVA showed a significant difference between the mean values, post-hoc pairwise comparisons were conducted to identify which pairs of means were significantly different from each other. For the pair-wise comparison, a Tukey's honestly significant difference (Tukey's HSD) test was adopted.

To determine the detection performance metrics of visual interpretations, bin numbers were used for the criterion for determining true positive (TP), false positive (FP), true negative (TN) and false negative (FN) values as shown in Table 1. For example, setting criterion to bin 2 (i.e., 2ng/ml) implies that a THC concentration of more than 2 ng/ml should be considered as a positive reading. That is, if a 0 or 2 ng/ml LFA is placed in bins #1 or 2, then it is considered as TN; if such LFA is placed in any of bins #3-6 a FP reading is produced. Conversely, if LFA with concentration more than 2 ng/ml is placed in bins # 3-6 then it is considered as TP; however, if such LFA is placed in bin # 1 or 2 a FN reading is produced. Using these data, sensitivity, specificity, accuracy, positive predictive value (PPV) and negative predictive value (NPV) were calculated at each criterion as:

$$\text{Sensitivity} = \frac{TP}{\text{TP} + \text{FN}} \quad \text{Specificity} = \frac{TN}{\text{TN} + \text{FP}}$$

$$\text{Accuracy} = \frac{TP + TN}{\text{TP} + \text{FP} + \text{TN} + \text{FN}} \quad \text{PPV} = \frac{TP}{\text{TP} + \text{FP}} \quad \text{NPV} = \frac{TN}{\text{TN} + \text{FN}}$$

Table 1. Four possible outcomes: true positive (TP), true negative (TN), false positive (FP), false negative (FN) at different criterion/cut-off levels (i.e., bin numbers)

Criterions	LFA concentrations	LFA placed in bin numbers					
		1	2	3	4	5	6
1	0	TN	FP				
	2,5,7.5,10 &25	FN	TP				
2	0 & 2	TN		FP			
	5,7.5,10 &25	FN		TP			
3	0,2 & 5	TN			FP		
	7.5, 10 & 25	FN			TP		
4	0,2, 5& 7.5	TN				FP	
	10 & 25	FN				TP	
5	0,2, 5,7.5 &10	TN					FP
	25	FN					TP

To determine the detection performance metrics of LIT, 50% of the LFAs in each concentration were randomly selected as a training/calibration set, and the remaining 50% of the LFAs were considered as a test set. The highest and lowest amplitude values of training set LFAs specified the range of bins in each concentration. After identifying bins, the amplitude value of a test LFA was compared to those of the bins at each concentration. A test LFA with amplitude value within the range of the bin was placed in the same concentration bin whereas the test LFA with amplitude value outside the range of the bin was considered to go to either higher or lower concentration bins; that is, if the amplitude was greater than that of the bin of the same concentration, then it was placed in the lower concentration bins while if the amplitude was lower than that of the bin then it was placed in the higher concentration bins. After assigning all LFAs to appropriate bins, TP, FP, TN, and FN values were calculated using the approach shown in Table 1.

Biomedical Optics EXPRESS

A receiver operating characteristic curve (ROC curve) was plotted to compare the detection performances of visual and LIT interpretations in distinguishing between the LFAs with THC and LFAs with no THC. The area under the ROC curve (AUC) that is considered as an effective measure of accuracy was also calculated for quantitative comparisons.

3. Results

3.1. Lock-in thermography interpretation of LFAs

Figure 3(a) depicts visual and LIT images of 6 representative LFAs at various THC concentrations. A decrease in the signal at the test lines is observed with the increase in THC concentrations in both visual and LIT images. However, LIT images show a better change in contrast of the test line as the concentration of THC increases compared to the contrast change in visual images. In LIT images, the test line of 5ng/ml (if not also 2 ng/ml) can be visually differentiated from the test lines of higher concentrations; however, it is very difficult to make such differentiation in visual images. For quantitative analysis, the normalized amplitude metric discussed in section 2.2 was calculated for all LFAs. Figure 3(b) shows the normalized amplitude values obtained from the representative LFAs of Fig. 3(a). The difference in the peak values of the curves at the test line is clearly observed for each pair of concentrations. To examine repeatability, the coefficient of variation (CV) was calculated using the 5 repeated measurements of each LFA. The CV is the ratio of the standard deviation and the overall mean, usually expressed as a percentage [37]. The averaged CV obtained from all the LFAs at all different concentrations was 2.03%, demonstrating high repeatability of LIT measurements.

Figure 3(c) displays the distribution of all the normalized amplitude values ($n = 300$: 6 concentrations $\times$ 10 LFAs/concentration $\times$ 5 repeated measurement of each LFA). Each box shows the normalized amplitude values of the 50 measurements carried out at a given concentration. The box plot shows no overlap in the distribution of data between any two concentration groups. Accordingly, the mean normalized amplitude values with 99% confidence interval error bars (Fig. 3(d)) show no overlap between any two concentration groups. One-way ANOVA test showed statistical significance between the mean normalized amplitude values of different concentration groups ($p < 0.001$). Tukey's pairwise comparisons showed that all the pairwise group comparisons were significantly different ($p < 0.001$). The effect size of 0.97 and statistical power of 1.0 was obtained at a significance level of 0.01 using a sample size of 50 in each concentration group.

Figure 4(a) shows the percentage of LFAs in each bin after splitting them into the training and test sets as described in Section 2.4. The sensitivity, specificity, accuracy, PPV, and NPV calculated from LIT data are shown in Table 2. The red solid line in Fig. 4(c) represents the ROC curve plotted from the LIT data. The area under the ROC curve (AUC) was found to be 0.99.

Table 2. Sensitivity, specificity, accuracy, positive predictive value (PPV) and negative predictive value (NPV) calculated from the visual and LIT interpretation of LFAs at various criterion/cut-off.

Positive reading criterion (ng/ml)	Sensitivity		Specificity		Accuracy		PPV		NPV	
	LIT	Visual	LIT	Visual	LIT	Visual	LIT	Visual	LIT	Visual
≥ 2	0.96	0.68	0.96	0.38	0.96	0.53	0.96	0.52	0.96	0.54
≥ 5	0.96	0.60	1	0.65	0.98	0.62	1	0.63	0.96	0.62
≥ 7.5	0.96	0.47	1	0.86	0.98	0.66	1	0.77	0.96	0.62
≥ 10	0.97	0.88	1	1	0.98	0.94	1	1	0.97	0.90
≥ 25	0.96	0.45	1	1	0.98	0.73	1	1	0.96	0.65

Biomedical Optics EXPRESS

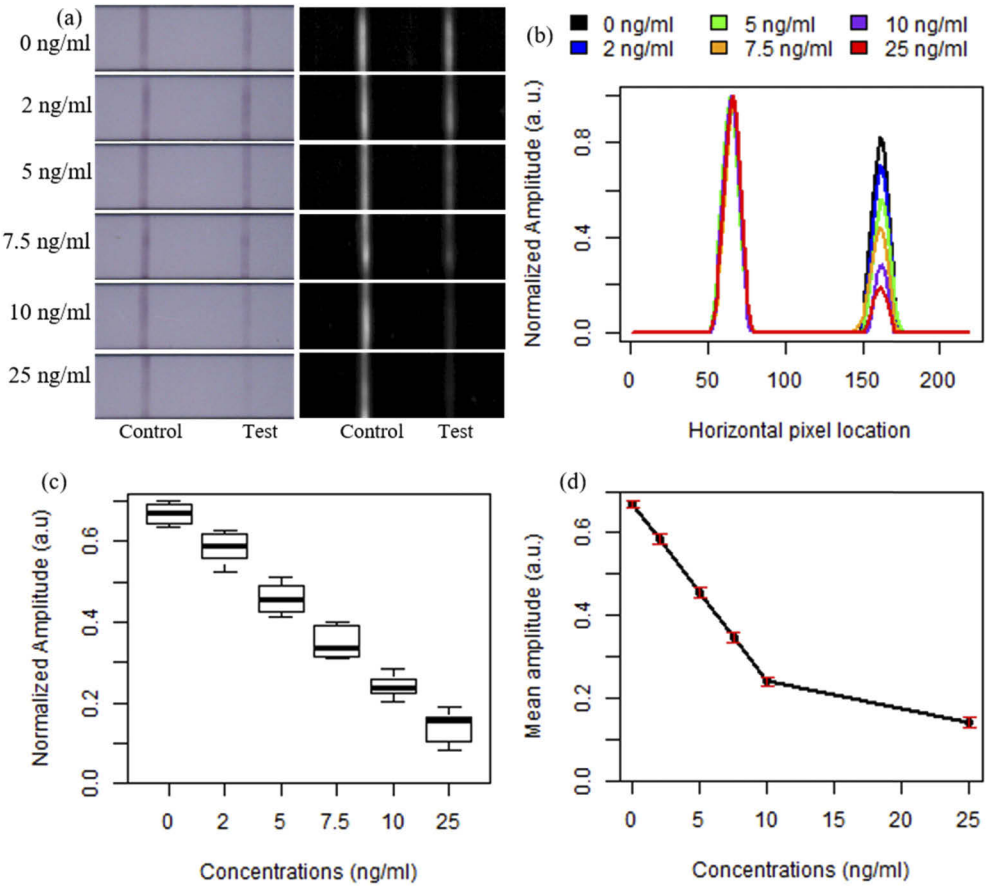

Fig. 3. (a) Visual and LIT images of 6 representative LFAs at concentrations of 0, 2, 5, 7.5, 10 and 25 ng/ml. (b) Normalized amplitude values obtained from LIT LFA images in (a). (c) Distribution of the entire dataset of the LFAs at various concentrations obtained from the LIT system. (d) Mean normalized amplitude at different THC concentrations obtained from (c) with 99% confidence interval error bars.

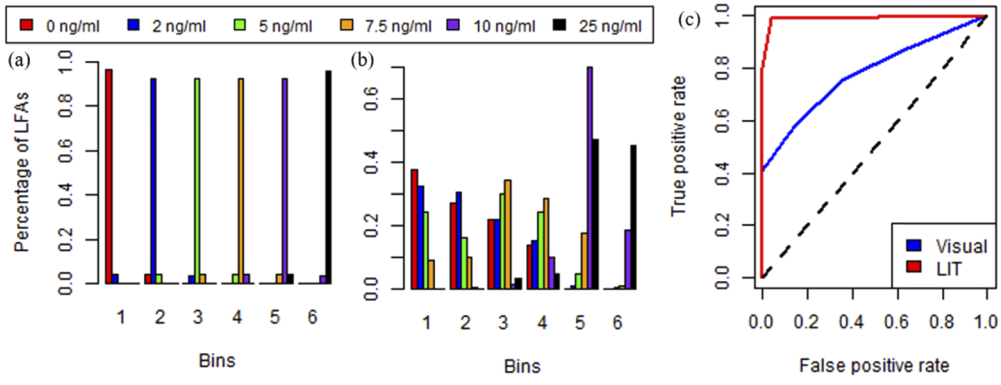

Fig. 4. Percentage of LFAs of various concentrations dropped in bin number 1-6 in LIT (a) and visual interpretation (b). (c) ROC curves from the visual and LIT interpretation data.

Biomedical Optics EXPRESS

3.2. Visual interpretation of LFAs

Forty-eight spiked LFAs were interpreted by 30 participants, as described in Section 2.3. Figure 4(b) shows the percentage of LFAs of various concentrations dropped in bin numbers 1-6 by all 30 participants. The corresponding sensitivity, specificity, accuracy, PPV, and NPV are shown in Table 2. The solid blue plot in Fig. 4(c) shows the ROC curve corresponding to the visual interpretation data. The area under the ROC curve was found to be 0.78.

4. Discussion and conclusion

In this study, LFA strips for THC saliva test were spiked at various concentrations of THC and inspected visually by adults and a LIT imaging system. Figure 3(a) depicts visual images of 6 representative LFAs at various concentrations. At high THC concentrations (e.g., 25 ng/ml), THC binds effectively with the antibodies present in the LFA sample pad; therefore, the antigen immobilized at the test line is unable to restrain with antibody conjugate, preventing the GNPs from being fixed on the test line and yielding lack of signal at the test line. However, at lower THC concentrations (e.g., between 2 and 10 ng/ml), some of the antibody conjugates are able to bind with antigen immobilized at the test line, thus forming a faint test line. At low THC concentrations (e.g., less than 7.5 ng/ml) the change in contrast with the decrease of concentration becomes small, making the classification of LFA with THC and without THC challenging. Accordingly, in visual interpretation (Fig. 4(b)) participants could not find the difference between the LFAs of concentrations less than 10 ng/ml; however, their diagnostic performance increased for LFA concentrations 10 ng/ml and higher. This indicates that THC concentrations of 10 ng/ml and 25 ng/ml were determined as a positive test by participants with higher accuracy. The sensitivity, specificity and accuracy values for identifying THC concentrations of 10ng/ml and more are 0.88, 1 and 0.94, respectively (Table 2). However, these values are less than 80% for identifying concentration less than 10 ng/ml and, as such, could not meet the Driving Under Influence of Drugs, Alcohol and Medicines (DRUID) standard of >80% sensitivity, specificity and accuracy at nominal detection threshold [38]. Similarly, PPV (i.e. probability of a positive reading being correct) and NPV (i.e. probability of a negative reading being correct) are crucial indicators of performance for a drug screening device at the roadside and workplace. These values are less than 80% for identifying THC concentrations of less than 10 ng/ml for visual interpretation. Therefore, based on the results depicted in Table 2 one can assume a detection threshold of 10ng/ml for visual interpretation of LFAs used in this study. We, however, anticipate this visual interpretation detection performance and threshold to deteriorate in practice because our participants were visually healthy young adults (20-35 years) with no history of eye surgery, color blindness, and visual impairment but at roadside or workplace tests are usually interpreted by individuals of different ages. Furthermore, since our visual tests were conducted in a well-illuminated room, we anticipate that the reliability of visual interpretation results to decline in practice due to suboptimal lighting conditions, such as roadside conditions at nighttime or in bad weather. Therefore, visual interpretation results suggest that if LFAs are, visually, interpreted by an objective and unbiased reader at roadside, detection of THC concentrations at *per se* limit (~1-5 ng/ml) is extremely unlikely and that one should expect inconsistent and unreliable readings when THC concentrations are above *per se* limit but lower than 10 ng/ml (if not 25 ng/ml).

Figure 3(a) depicts LIT images of 6 representative LFAs at various concentrations. Qualitative analysis of these images (Fig. 3(b)) suggests that, unlike visual images, the contrast of the test line in LIT is very sensitive to change in THC concentration. Better sensitivity of LIT can be attributed to the fact that LIT utilizes the diffusion of thermal waves to interrogate the entire thickness of LFAs whereas the scattered light in visual interpretation originates predominantly form surface (and superficial layer) of LFA [30]. That is, in LIT the contributions of all the GNPs located within the thermal diffusion length are integrated and accounted for in the normalized

Biomedical Optics EXPRESS

amplitude values. Figure 3(d) depicts the mean normalized amplitude values within the test band for stripes with different THC concentrations. The mean normalized amplitude value decreases monotonically with an increase in the THC concentrations in the sample. The mean normalized amplitude values were statistically different ($p < 0.001$) between all the THC concentrations used in this study. The post-hoc pair-wise comparison shows that the LIT can reliably differentiate LFA spiked at 2 ng/ml from those spiked at 0 ng/ml. Table 2 shows that LIT technology can differentiate THC concentrations of 2 ng/ml and more from 0 ng/ml with sensitivity, specificity, and accuracy of 96% that is considerably higher than the standard set by DRUID for nominal detection threshold of a drug screening device [38]. Also, the predictive values (i.e. PPV and NPV) are almost 100% at 2 ng/ml which implies the outstanding confidence that one can have in LIT technology results. These experimental results and statistical analyses suggest that interrogation of the thermal signature of GNPs from the entire thickness of the LFAs significantly improves the detection threshold of commercially available LFAs (2 ng/ml vs. the nominal 25 ng/ml limit).

The area under the ROC curve plotted from the LIT data is considerably higher than that of the visual interpretation data (0.99 vs 0.78). This indicates that the diagnostic performance of LIT is better than visual interpretation for distinguishing LFAs spiked with THC and without THC. Another interesting aspect of the developed LIT system is its potential for quantifying THC concentration. Since the box plots of any two concentrations do not overlap (Fig. 3(c)), this imaging modality can use data of Fig. 3(d) as calibration to provide an accurate prediction for THC concentration in oral fluid.

The performance can be improved even more by adopting better lateral flow immunoassay assembly approaches. As can be seen in Fig. 3(c), there is a high degree of variability among the LFAs of the same concentrations. This may be due to the batch processing approach used in the LFA assembly. The batch processing approach involves a high degree of manual labor and can be prone to product variability [39]. Another approach for improving performance is the use of a green laser beam (wavelength ~ 550 nm) instead of the near-infrared laser (808nm). Our spectral measurements show that the difference in the absorption of light between the test line and the surrounding nitrocellulose paper is maximum at a wavelength of 550 nm. However, the shorter-wavelength lasers are typically more expensive and hence not suitable for commercialization. We are currently exploring the replacement of the 808nm laser with an assembly of high-power green LEDs.

In conclusion, we have developed a lock-in thermography imaging system to demonstrate the detection and quantification of THC in the oral fluid at unprecedented low concentrations. Our results suggest that LIT interrogation of low-cost commercial LFAs allows for more than an order of magnitude improvement in the detection threshold. We have also compared the performance of our LIT reader with visual interpretation. Results suggest a significant improvement in detection threshold and accuracy when using LIT. Based on the DRUID definition, the detection threshold of visual interpretation in our study is 10 ng/ml with 94% accuracy whereas the detection threshold of LIT is 2 ng/ml at 96% accuracy. The 2ng/ml detection threshold of developed LIT technology is significantly better than any of the workplace or roadside on-site THC screening solutions currently available in the market (e.g., Dräger DrugTest) [38,40]. We are currently pursuing commercialization of the developed technology and anticipate it to be used in testing cannabis consumption in various application fields, such as testing (a) drivers in the roadside for investigating driving under the influence of cannabis and drug-related accidents (b) employees to ensure workplace safety (c) patients in hospitals who uses cannabis for pain relief and/or sleep improvement (d) players in competitions who uses cannabis to enhance athletic performance (e) correlation of THC with human cognitive and motor functions and (f) cannabis manufacturing plans for quality control purposes. Besides the detection of THC, LFAs are routinely used for the detection of pathogenic bacteria in food and water [41–42], disease biomarkers such as

Biomedical Optics EXPRESS

foot-and-mouth disease virus [43], extraparenchymal neurocysticercosis [44], and cancer and cardiac markers in various biofluids. Since a significant majority of LFAs are based on GNPs, the developed LIT reader can potentially be used for sensitive and quantitative interpretation of results in such delicate application. The most important limitation of our thermo-photonic system is the cost and size of instrumentation. The cost of our system is mostly determined by the cost of the infrared camera (approximately $7,000 USD for the camera used in this study). However, we have recently shown that the cost and size limitation can be significantly reduced by using cell-phone attachment infrared cameras [45]. Development of a portable system using low-cost ($250) cell-phone attachment infrared cameras for the detection and quantification of THC in oral fluid is in progress in our lab. We anticipate that the low-cost and portable thermo-photonic imager promises an affordable solution that allows for proper enforcement of *per se* regulations worldwide.

Funding

Natural Sciences and Engineering Research Council of Canada (I2IPJ 531925-18, RGPIN-2015-03666); Canada First Research Excellence Fund (CFREF, Vision: Science to Application).

Acknowledgments

N.T. is grateful to the Natural Sciences and Engineering Research Council of Canada for the award of Discovery and Idea2Innovation Grants, to the Vision: Science to Applications (VISTA) program for the award of Prototyping fund, and to Innovation York for their support.

Disclosures

The authors declare that there are no conflicts of interest related to this article. This study was presented in the SPIE Photonics West Conference (San Francisco, CA, United States) on 3 Feb 2020 in the "Optical Diagnostics and Sensing XX: Toward Point-of-Care Diagnostics" session.

References

1. Public Safety Canada. Cannabis Policy Performance Metrics, Research Summary 2016, Ottawa, Ontario.
2. World Health Organization Reports. Management of substance abuse: Cannabis. https://www.who.int/substance_abuse/facts/cannabis/en/.
3. W. C. Kerr, Y. Ye, M. S. Subbaraman, E. Williams, and T. K. Greenfield, "Changes in Marijuana Use Across the 2012 Washington State Recreational Legalization: Is Retrospective Assessment of Use Before Legalization More Accurate?" J. Stud. Alcohol Drugs **79**(3), 495–502 (2018).
4. Shikha Prashad and Francesca M. Filbey. "Cognitive motor deficits in cannabis users," Feb. 2017. Current Opinion in Behavioral Sciences.
5. Poling Sewell, and Sofuoglu. See also: Brooks-Russell, Wempe, Vigil, et al. "Marijuana use and driving: Systematic literature review," 2017. Colorado Department of Public Health and Environment.
6. Ole Rogeberg and Rune Elvik. "The effects of cannabis intoxication on motor vehicle collision revisited and revised," Feb. 2016. Addiction.
7. Jean-Louis Martin, Blandine Gadegbeku, and Dan Wu, *et al.*, "Cannabis, alcohol, and fatal road accidents," 2017. PLoS One. In comparison, the study found that drivers under the influence of alcohol are 17.8 times more likely to be culpable for a fatal accident.
8. European Monitoring Centre for Drugs and Drug Addiction (2019), European Drug Report 2019: Trends and Developments, Publications Office of the European Union, Luxembourg
9. Canadian Centre on Substance Use and Addiction 2018, "Canadian drug summary: cannabis"
10. European Monitoring Centre for Drugs and Drug Addiction, "The state of the drugs problem in Europe," Annual report 2012.
11. D. J. Beirness and A. J. Porath-Waller, "Clearing the smoke on cannabis: Cannabis use and driving-an update," Canadian Centre on Substance Abuse" (2019).
12. Substance Abuse and Mental Health Services Administration, "The National Survey on Drug Use and Health: 2017"
13. Australian Institute of Health and Welfare 2017. National Drug Strategy Household Survey 2016: detailed findings. Drug Statistics series no. 31. Cat. no. PHE 214. Canberra: AIHW

Biomedical Optics EXPRESS

14. R. L. Hartman, T. L. Brown, G. Milavetz, A. Spurgin, D. A. Gorelick, G. R. Gaffney, and M. A. Huestis, "Effect of blood collection time on measured Δ9-tetrahydrocannabinol concentrations: implications for driving interpretation and drug policy," Clin. Chem. **62**(2), 367–377 (2016).
15. D. J. Beirness and D. R. Smith, "An assessment of oral fluid drug screening devices," J. - Can. Soc. Forensic Sci. **50**(2), 55–63 (2017).
16. M. A. Huestis and E. J. Cone, "Relationship of Δ9-Tetrahydrocannabinol Concentrations in Oral Fluid and Plasma after Controlled Administration of Smoked Cannabis," J. Anal. Toxicol. **28**(6), 394–399 (2004).
17. G. Li, S. P. Baker, Q. Zhao, J. E. Brady, B. H. Lang, G. W. Rebok, and C. DiMaggio, "Drug violations and aviation accidents: findings from the US mandatory drug testing programs," Addiction **106**(7), 1287–1292 (2011).
18. M. T. French, M. C. Roebuck, and P. K. Alexandre, "To test or not to test: do workplace drug testing programs discourage employee drug use?" Soc. Sci. Res. **33**(1), 45–63 (2004).
19. S. George, "A snapshot of workplace drug testing in the UK," Occup. Med. **55**(1), 69–71 (2005).
20. O. A. Silva and M. Yonamine, "Drug abuse among workers in Brazilian regions," Rev. Saude Publica **38**(4), 552–556 (2004).
21. E. J. Cone, L. Presley, M. Lehrer, W. Seiter, M. Smith, K. W. Kardos, D. Fritch, S. Salamone, and R. S. Niedbala, "Oral fluid testing for drugs of abuse: positive prevalence rates by Intercept™ immunoassay screening and GC-MS-MS confirmation and suggested cutoff concentrations," J. Anal. Toxicol. **26**(8), 541–546 (2002).
22. S. Macdonald, W. Hall, P. Roman, T. Stockwell, M. Coghlan, and S. Nesvaag, "Testing for cannabis in the work-place: a review of the evidence," Addiction **105**(3), 408–416 (2010).
23. H. Choi, S. Baeck, E. Kim, S. Lee, M. Jang, J. Lee, H. Choi, and H. Chung, "Analysis of cannabis in oral fluid specimens by GC-MS with automatic SPE," Sci. Justice **49**(4), 242–246 (2009).
24. M. Sánchez, A. Arroyo, M. Barbal, M. Palahí, and A. Mora, "Cozart® RapiScan Oral Fluid Drug Testing System validation by GC-MS/MS analysis," Ann. Toxicol. Anal. **20**(3), 131–136 (2008).
25. V. Reinstadler, S. Lierheimer, M. Boettcher, and H. Oberacher, "A validated workflow for drug detection in oral fluid by non-targeted liquid chromatography-tandem mass spectrometry," Anal. Bioanal. Chem. **411**(4), 867–876 (2019).
26. O. Quintela, D. M. Andrenyak, A. M. Hoggan, and D. J. Crouch, "A validated method for the detection of Δ9-tetrahydrocannabinol and 11-nor-9-carboxy-Δ9-tetrahydrocannabinol in oral fluid samples by liquid chromatography coupled with quadrupole-time-of-flight mass spectrometry," J. Anal. Toxicol. **31**(3), 157–164 (2007).
27. D. J. Crouch, J. M. Walsh, L. Cangianelli, and O. Quintela, "Laboratory evaluation and field application of roadside oral fluid collectors and drug testing devices," Ther. Drug Monit. **30**(2), 188–195 (2008).
28. B. D. Plouffe and S. K. Murthy, "Fluorescence-based lateral flow assays for rapid oral fluid roadside detection of cannabis use," Electrophoresis **38**(3-4), 501–506 (2017).
29. P. Rezai, N. Tabatabaei, and A. Ojaghi, "System and method for photo-thermal analysis of immunoassay tests," U.S. Patent Application 15/839,325, filed May 23, 2019.
30. A. Ojaghi, M. Pallapa, N. Tabatabaei, and P. Rezai, "High-sensitivity interpretation of lateral flow immunoassays using thermophotonic lock-in imaging," Sens. Actuators, A **273**, 189–196 (2018).
31. K. M. Koczula and A. Gallotta, "Lateral flow assays," Essays Biochem. **60**(1), 111–120 (2016).
32. Canadian Society of Forensic Science Drugs and Driving Committee (DDC) Drug Screening Equipment – Oral Fluid Standards and Evaluation Procedures.
33. N. Tabatabaei, A. Mandelis, and B. T. Amaechi, "Thermophotonic lock-in imaging of early demineralized and carious lesions in human teeth," J. Biomed. Opt. **16**(7), 071402 (2011).
34. N. Tabatabaei, A. Mandelis, M. Dehghany, K. H. Michaelian, and B. T. Amaechi, "On the sensitivity of thermophotonic lock-in imaging and polarized Raman spectroscopy to early dental caries diagnosis," J. Biomed. Opt. **17**(2), 025002 (2012).
35. A. Ojaghi, A. Parkhimchyk, and N. Tabatabaei, "First step toward translation of thermophotonic lock-in imaging to dentistry as an early caries detection technology," J. Biomed. Opt. **21**(9), 096003 (2016).
36. E. B. Shokouhi, M. Razani, A. Gupta, and N. Tabatabaei, "Comparative study on the detection of early dental caries using thermo-photonic lock-in imaging and optical coherence tomography," Biomed. Opt. Express **9**(9), 3983–3997 (2018).
37. J. M. Bland and D. G. Altman, "Statistical notes: measurement error proportional to the mean," BMJ **313**(7049), 106 (1996).
38. H. Schulze, M. Schumacher, R. Urmeew, K. Auerbach, J. Alvarez, and I. M. Bernhoft, *et al.*, "Findings from the DRUID project Driving Under the Influence of Drugs, Alcohol, and Medicines in Europe d findings from the DRUID project," Lisbon: EMCDDA (2012).
39. Innova Biosciences Ltd, A guide to lateral flow immunoassays, Babraham Research Campus, Cambridge.
40. T. R. Arkell, R. C. Kevin, J. Stuart, N. Lintzeris, P. S. Haber, J. G. Ramaekers, and I. S. McGregor, "Detection of Δ9 THC in oral fluid following vaporized cannabis with varied cannabidiol (CBD) content: An evaluation of two point-of-collection testing devices," Drug Test. Anal. **11**(10), 1486–1497 (2019).
41. Y. Zhao, H. Wang, P. Zhang, C. Sun, X. Wang, X. Wang, R. Yang, C. Wang, and L. Zhou, "Rapid multiplex detection of 10 foodborne pathogens with an up-converting phosphor technology-based 10-channel lateral flow assay," Sci. Rep. **6**(1), 21342 (2016).
42. J. Hwang, D. Kwon, S. Lee, and S. Jeon, "Detection of Salmonella bacteria in milk using gold-coated magnetic nanoparticle clusters and lateral flow filters," RSC Adv. **6**(54), 48445–48448 (2016).

Biomedical Optics EXPRESS

43. K. O. Jae, N. P. Ferris, K. N. Lee, Y. S. Joo, B. H. Hyun, and J. H. Park, "Simple and rapid lateral-flow assay for the detection of foot-and-mouth disease virus," Clin. Vaccine Immunol. **16**(11), 1660–1664 (2009).
44. A. Fleury, P. Sastre, E. Sciutto, S. Correia, A. Monedero, A. Toledo, M. Hernandez, L. J. S. Harrison, and R. M. E. Parkhouse, "A lateral flow assay (LFA) for the rapid detection of extraparenchymal neurocysticercosis using cerebrospinal fluid," Exp. Parasitol. **171**, 67–70 (2016).
45. M. Razani, A. Parkhimchyk, and N. Tabatabaei, "Lock-in thermography using a cellphone attachment infrared camera," AIP Adv. **8**(3), 035305 (2018).